Lattice Boltzmann simulations of a dumbbell moving in a Poiseuille flow



2007 Chinese Phys. 16 2444

(http://iopscience.iop.org/1009-1963/16/8/048)

Vol 16 No 8, August 2007
1009-1963/2007/16(08)/2444-05

Chinese Physics



# Lattice Boltzmann simulations of a dumbbell moving in a Poiseuille flow*

Yi Hou-Hui(伊厚会)[a)b)†], Chen Yan-Yan(陈艳燕)[a)b)], and Li Hua-Bing(李华兵)[a)c)]

[a)] *Shanghai Institute of Applied Physics, Chinese Academy of Sciences, Shanghai* 201800, *China*
[b)] *Graduate School of the Chinese Academy of Sciences, Beijing* 100080, *China*
[c)] *Department of Information Material Science and Engineering,*
*Guilin University of Electronic Technology, Guilin* 541004, *China*

(Received 9 October 2006; revised manuscript received 20 November 2006)

In this paper, the lattice Boltzmann method is applied to simulate a dumbbell moving in a pressure-driven flow in a planar channel with the stress-integration method for the evaluation of hydrodynamic force acting on the cylinders. The simulation results show that the dumbbell also has the important feature of the Segré–Silberberg effect like a particle in a Poiseuille flow. The dumbbell trajectories, orientations, the cylinders vertical velocities and angular velocities all reach their equilibrium values separately independent of their initial positions. It is also found that the dumbbell equilibrium positions depend on the flow Reynolds number, blockage ratio and elastic coefficient. This study is expected to be helpful to understand the dynamics of polymer solutions, polymer synthesis and reaction, etc.

**Keywords:** lattice Boltzmann method, dumbbell
**PACC:** 4755

## 1. Introduction

Studying the properties of polymers[1−3] is of great importance because they are ubiquitous and usually used in the food, gene transfection, drug delivery, pharmaceuticals, coating, and chemical industries, etc. Some properties of the polymers are often governed by their conformations and the interactions between the molecules and the solvents. Due to the complexity of the polymers themselves, their configurations are often simplified as the dumbbell model[4−7] to understand the mechanism of the polymers. In this paper, we will concentrate on the study of the behaviour of the dumbbell in the fluid flows.

Recently, the solid–fluid two-phase flow system has been extensively studied both theoretically and experimentally, and surprising achievement has been obtained.[8−13] In the past fifteen years, the lattice Boltzmann method[14−17] has been proven as an alternative numerical method for simulating fluid flows in various physical and engineering systems, especially in the areas of complex fluids such as particle suspension flows,[18−24] binary mixtures,[25−29] flow in porous media[30−34] and blood flows.[35−40] Ladd was the first to apply the lattice Boltzmann method to simulate particle suspensions, and the hydrodynamic force exerted on solid particles was computed by momentum exchange method.[18] Based on this method, the sedimentations of charged cylinder,[19] elliptic cylinder[20,21] and dumbbell[22] were studied numerically in a two-dimensional channel. Li *et al*[23] used the stress-integration method to evaluate hydrodynamic force exerted on solid particles in fluid in two dimensions. The accuracy of this scheme has been demonstrated by simulating the sedimentation of a circular cylinder in a vertical channel and comparing the simulation results with those obtained from a second-order finite-element scheme. The migration of a neutrally buoyant circular cylinder in a Poiseuille flow was also studied by this method.

In this paper, the lattice Boltzmann method is extended to study the dumbbell moving in a pressure-driven Poiseuille flow in two dimensions. The dumbbell trajectories, time-dependent orientations, the time-dependent vertical velocities and angular velocities are computed numerically. Effects of parameters controlling the particle motion, which are flow Reynolds number, blockage ratio and elastic coefficient, are also investigated extensively.

This paper is organized as follows. In Section 2

*Project supported by the National Natural Science Foundation of China (Grant Nos 10474109 and 10447001) and the Foundation of Ministry of Personnel of China.
†E-mail: houhuily@163.com

we briefly describe the lattice Boltzmann method. We present our simulation results in Section 3. The conclusions are given in Section 4.

## 2. The lattice Boltzmann model

We choose to work on a two-dimensional square lattice with nine velocities. Let $f_i(\boldsymbol{x}, t)$ be a non-negative real number describing the distribution function of the fluid density at site $\boldsymbol{x}$ and time $t$ moving in direction $\boldsymbol{e}_i$. Here $\boldsymbol{e}_0 = (0, 0)$, $\boldsymbol{e}_i = (\cos\pi(i-1)/2, \sin\pi(i-1)/2)$, for $i = 1, 2, 3, 4$, and $\boldsymbol{e}_i = \sqrt{2}(\cos\pi(2i-1)/4, \sin\pi(2i-1)/4)$, for $i = 5, 6, 7, 8$ are the nine possible velocity vectors. The distribution functions evolve according to a Boltzmann equation which is discrete in both space and time,[15,16]

$$f_i(\boldsymbol{x} + \boldsymbol{e}_i, t + 1) - f_i(\boldsymbol{x}, t) = -\frac{1}{\tau}(f_i - f_i^{\rm eq}). \qquad (1)$$

The density $\rho$ and macroscopic velocity $\boldsymbol{u}$ are defined by

$$\rho = \sum_i f_i, \qquad \rho\boldsymbol{u} = \sum_i f_i \boldsymbol{e}_i, \qquad (2)$$

and the equilibrium distribution functions $f_i^{\rm eq}$ are usually supposed to be dependent only on the local density $\rho$ and flow velocity $\boldsymbol{u}$. A suitable choice is[15,16]

$$f_i^{\rm eq} = \rho\alpha_i\Big[1 + 3\boldsymbol{e}_i\cdot\boldsymbol{u} + \frac{9}{2}(\boldsymbol{e}_i\cdot\boldsymbol{u})^2 - \frac{3}{2}u^2\Big], \qquad (3)$$

where $\alpha_0 = 4/9$, $\alpha_1 = \alpha_2 = \alpha_3 = \alpha_4 = 1/9$, and $\alpha_5 = \alpha_6 = \alpha_7 = \alpha_8 = 1/36$. The macroscopic equations can be obtained by a Chapman–Enskog procedure.[15,16] They are the continuity equation

$$\partial_t\rho + \partial_\alpha(\rho u_\alpha) = 0, \qquad (4)$$

and the Navier–Stokes equations

$$\begin{aligned}&\partial_t(\rho u_\alpha) + \partial_\beta(\rho u_\alpha u_\beta)\\ &= \partial_\alpha p + \nu\partial_\beta[\rho(\partial_\alpha u_\beta + \partial_\beta u_\alpha)],\end{aligned} \qquad (5)$$

where $p$ and $\nu$ are the pressure and the viscosity, defined by the equations $p = c_s^2\rho$ with $c_s^2 = 1/3$ and $\nu = (2\tau - 1)/6$, respectively.

## 3. Results and discussion

Figure 1 displays the schematic diagram of a neutrally buoyant dumbbell moving in a Poiseuille flow in our lattice Boltzmann simulations. The width of the channel is $D = 1.0$ cm and the length of channel is $L = 4.0$ cm. The densities of the fluid and the dumbbell are both 1 g/cm$^3$ and the kinematic viscosity of the fluid is $\nu = 1.0\times10^{-2}$ cm$^2$/s, corresponding to that of water at 20 °C. The pressure drop from inlet to outlet is set to be $8.64\times10^{-2}$ Pa. The Reynolds number of the channel flow is defined as $Re = u_m D/2\nu$, where $u_m$ is the maximal velocity of the flow without any dumbbell in the channel and $\nu$ is the viscosity of the fluid. The two-dimensional dumbbell in our simulations consists of two identical neutrally buoyant cylinders with diameter $d$ connected by a massless spring. The blockage ratio is defined as $d/D$ and the elastic constant of the spring is denoted by $k$ and its free length is $l_0$. $l_0$ is always set to be 0.2 cm except for the discussion of the blockage ratio dependence in Section 3.3. The orientation of the dumbbell is defined as the angle $\theta$ between the line linked the centres of two cylinders and the horizon. In the lattice Boltzmann simulations, $\tau = 0.75$ and $D = 100$ lattice units separately. Initially the distribution functions at all the fluid nodes are set to be the equilibrium distribution functions with zero velocity except for those at inlet and outlet. The dumbbell is situated at rest with orientation $\theta = 90°$ and let the fluid flow develop and approach a steady state driven by pressure drop. When the time step reaches at 10 000, the dumbbell is released and will move in the Poiseuille flow. The inlet and outlet boundaries are always $L/2$ apart from the moving dumbbell.

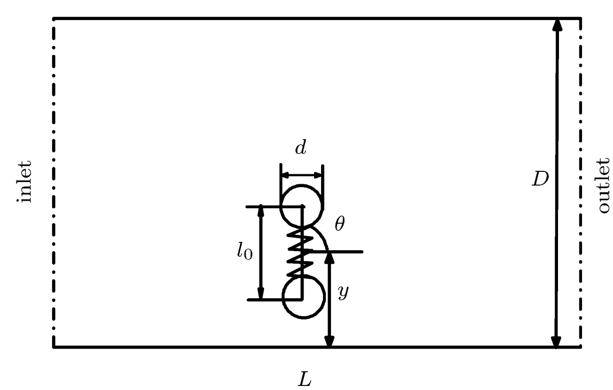


**Fig.1.** Schematic diagram of a neutrally buoyant dumbbell moving in a Poiseuille flow.

In our simulations, the boundary condition for the moving cylinders is treated by the method described in Refs.[23,37]. Periodical boundary condition proposed by Inamuro *et al* is implemented at inlet and outlet[41] to produce Poiseuille flow. The hydrodynamic force acting on two cylinders is evaluated based on the method of stress-integration.[23] The elastic force exerted on the two cylinders is assumed to obey Hooke's law, i.e.

$$F_{xi} = k\frac{(x_j - x_i)(l - l_0)}{l}, \quad (6)$$

$$F_{yi} = k\frac{(y_j - y_i)(l - l_0)}{l}, \quad (7)$$

where $i \neq j$, $i, j = 1, 2$, and $l$ is the length of the dumbbell. The translation and rotation of the two cylinders are updated at each Newtonian dynamics time step by using a so-called half-step 'leap-frog' scheme respectively.[42]

## 3.1. The motion of the dumbbell with different initial positions

Figure 2 displays the dumbbell centroidal trajectories (a), time-dependent orientations (b), the two cylinders time-dependent vertical velocities $v_y$ (c) and angular velocities $\omega$ (d) with different initial positions $y_{in}/D$. The Reynolds number, the elastic constant of the spring and blockage ratio are set to be $Re = 10.83$, $k = 7.2 \times 10^{-5}$ dyn/cm (1 dyn = $10^{-5}$N) and $d/D = 0.1$ respectively in our simulations. Figure 2(a) shows that the dumbbell migrates inwards when the dumbbell is placed near the wall, while outwards when the dumbbell is situated close to the channel centre initially. All of them settle a same equilibrium position between the channel centre and the channel wall. A cylinder (sphere) migrating in a Poiseuille flow also shares this feature,[23,43,44] which is called Segré–Silberberg effect. The orientations $\theta$ of the dumbbell also reach their equilibrium values as shown in Fig.2(b). Numerically the orientation of the dumbbell is 11.5°, which implies that the cylinder near the centre drags another cylinder forward. The vertical velocities $v_y$ and angular velocities $\omega$ of the two cylinders all reach their steady state separately independent of the dumbbell initial positions as shown in Figs.2(c) and 2(d). The magnitude of the angular velocity of the upper cylinder in steady state is smaller than that of the lower one.

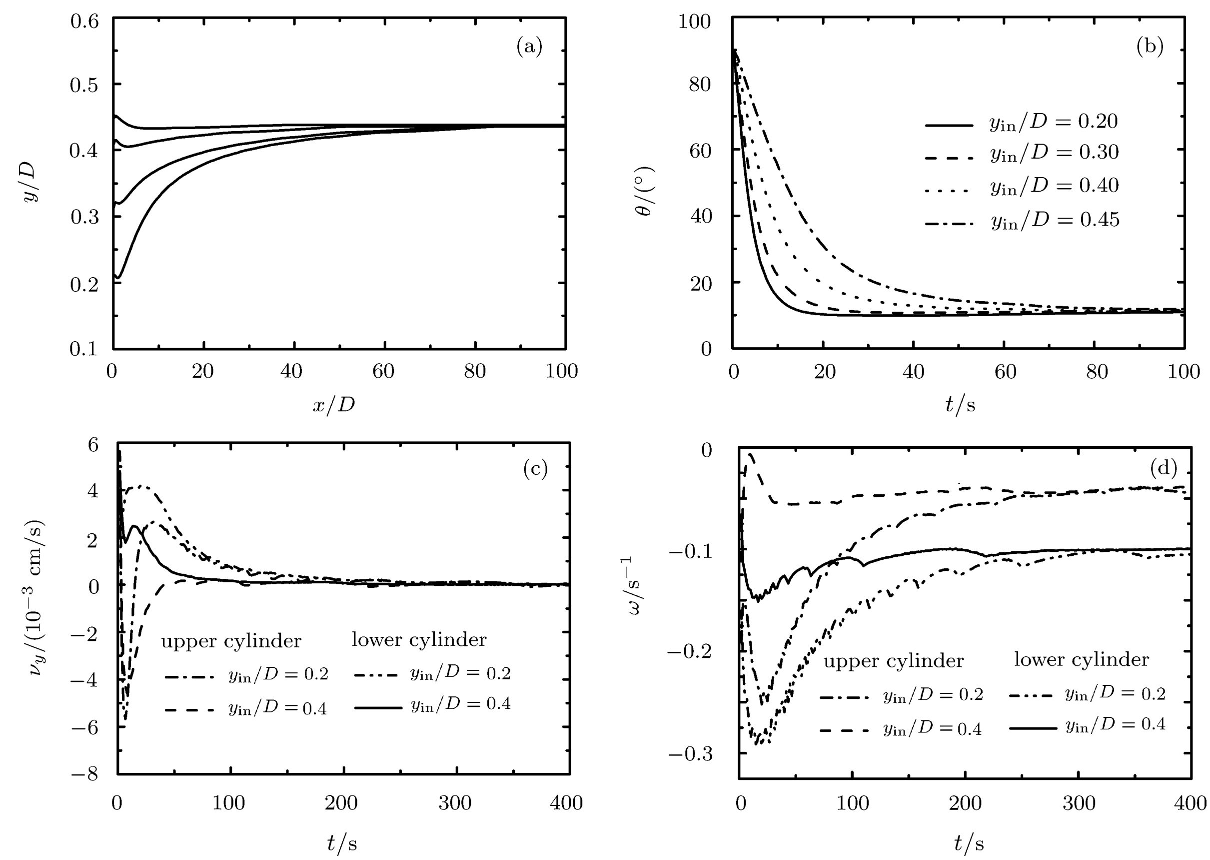


**Fig.2.** The centroidal trajectories (a), time-dependent orientations (b), time-dependent vertical velocities $v_y$ (c) and angular velocities $\omega$ (d) of the two cylinders of the dumbbell for different initial positions $y_{in}/D$ at $Re = 10.83$, $k = 7.2 \times 10^{-5}$ dyn/cm and $d/D = 0.1$.

### 3.2. The flow Reynolds number dependence of the dumbbell motion

Figure 3 displays the dumbbell equilibrium positions for different flow Reynolds numbers with elastic constant $k = 7.2 \times 10^{-5}$ dyn/cm and blockage ratio $d/D = 0.1$. It is clear that the dumbbell equilibrium positions keep almost invariably for flow Reynolds number $Re$ less than 10. The dumbbell equilibrium positions move towards the wall as the flow Reynolds numbers increase in case of $Re > 15$.

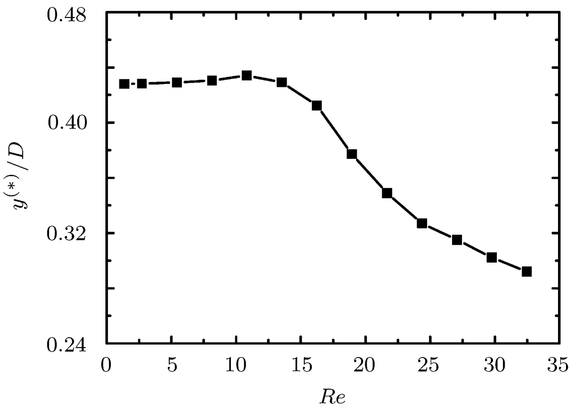


**Fig.3.** The equilibrium positions of the centroid of the dumbbell for different Reynolds numbers at $k = 7.2\times10^{-5}$ dyn/cm and $d/D = 0.1$.

### 3.3. The blockage ratio dependence of the dumbbell motion

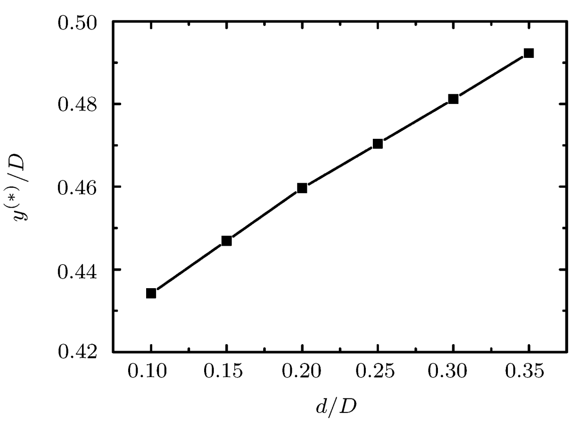


**Fig.4.** The equilibrium positions of the centroid of the dumbbell for different blockage ratios at $Re = 10.83$ and $k = 7.2 \times 10^{-5}$ dyn/cm.

Figure 4 displays the effect of blockage ratio $d/D$ on equilibrium position with a fixed flow Reynolds number $Re = 10.83$ and elastic constant $k = 7.2\times10^{-5}$ dyn/cm. The free length $l_0$ of the dumbbell is set to be 0.20 cm, 0.25 cm, 0.30 cm, 0.35 cm, 0.40 cm, 0.45 cm for $d/D = 0.10, 0.15, 0.20, 0.25, 0.30, 0.35$ respectively in order to keep sufficient space between the two cylinders. The simulation results show that the dumbbell equilibrium position $y^*/D$ increases as the blockage ratio $d/D$ increases and vice versa.

### 3.4. The elastic constant dependence of the dumbbell motion

Figure 5 displays the dumbbell equilibrium positions varying with the elastic constants $k$ at Reynolds number $Re = 10.83$ and blockage ratio $d/D = 0.1$. The numerical simulation results show that the dumbbell equilibrium position versus $k$ obeys an exponential decay, i.e. $y^*/D = 0.41 + 0.099\mathrm{e}^{-k/6.1}$. The difference of the dumbbell equilibrium position between $k = 2.88 \times 10^{-4}$ dyn/cm and $k = 2.16 \times 10^{-4}$ dyn/cm is less than 0.1%, implying that we can obtain the converged simulation results when $k$ is larger than $2.16 \times 10^{-4}$ dyn/cm. So a critical elastic constant $k_0 = 2.16 \times 10^{-4}$ dyn/cm is introduced. The larger elastic constant $k$ favours the dumbbell equilibrium position near the channel wall while smaller elastic constant $k$ favours the dumbbell equilibrium position near the channel centre on the condition of $k < k_0$.

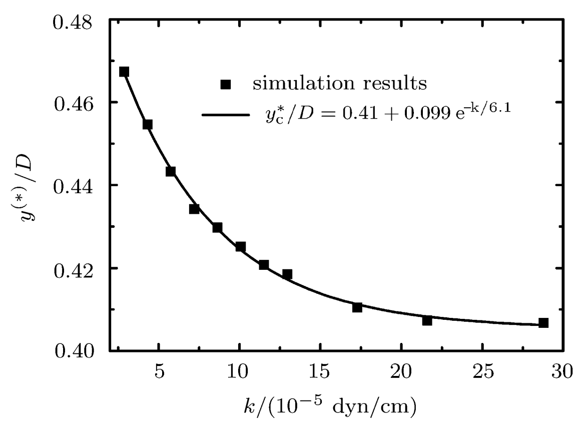


**Fig.5.** The equilibrium position of the centroid of the dumbbell versus $k$ at Reynolds number $Re = 10.83$ and blockage ratio $d/D = 0.1$.

## 4. Conclusion

We applied the lattice Boltzmann method to investigate the motion of the dumbbell in a pressure-driven Poiseuille flow with the hydrodynamic force exerted on the dumbbell computed by stress-integration method. The dumbbell trajectories, time-dependent orientations and time-dependent velocities and angular velocities of the components are studied numerically. The equilibrium values of the dumbbell positions, orientations, velocities and angular velocities of two cylinders are independent of their initial positions. It is also found that the dumbbell equilibrium position depends on the flow Reynolds number, blockage ratio and elastic coefficient.

Our study should be helpful in understanding the mechanism of the polymers, i.e. dynamics of polymer solutions, polymer synthesis and reaction, protein crystallization, etc. Because of the complexity of the polymers themselves, more models and factors must be considered to understand the properties of the polymers. We are working in this direction.

## Acknowledgement

We thank Professor Haiping Fang, and Dr Lijuan Zhang for helpful discussions and Shanghai Supercomputer Centre of China for support of the computation.

## References

[1] Perkins T T, Smith D E and Chu S 1997 *Science* **276** 2016
[2] Smith D E and Chu S 1998 *Science* **281** 1335
[3] Doi M and Edwards S F 1986 *The Theory of Polymer Dynamics* (Oxford: Clarendon)
[4] Jourdain B, Leliévre T and Bris C L 2002 *Math. Models Methods Appl. Sci.* **12** 1205
[5] Larson R G, Perkins T T, Smith D E and Chu S 1997 *Phys. Rev.* E **55** 1794
[6] Song X Y 2002 *Phys. Rev.* E **66** 011909
[7] Teixeira R E, Babcock H P, Shaqfeh E S G and Chu S 2005 *Macromolecules* **38** 581
[8] Hu H H, Joseph D D and Crochet M J 1992 *Theor. Comput. Fluid Dyn.* **3** 285
[9] Feng J, Hu H H and Joseph D D 1994 *J. Fluid Mech.* **261** 95
[10] Hu H H 1996 *Int. J. Multiphase Flow* **22** 335
[11] Crocker J C and Grier D G 1994 *Phys. Rev. Lett.* **73** 352
[12] Lin J Z, Li J, Zhu L and James A O 2005 *Chin. Phys.* **14** 1185
[13] Lin J Z, Li J and Zhang W F 2005 *Chin. Phys.* **14** 2529
[14] McNamara G R and Zanetti G 1988 *Phys. Rev. Lett.* **61** 2332
[15] Qian Y H, d'Humiéres D and Lallemand P 1992 *Europhys. Lett.* **17** 479
[16] Chen S, Chen H, Martinez D O and Matthaeus W H 1991 *Phys. Rev. Lett.* **67** 3776
[17] Chen H, Chen S and Matthaeus W H 1992 *Phys. Rev.* A **45** 5339
[18] Ladd A J C 1994 *J. Fluid Mech.* **271** 285
[19] Wan R Z, Fang H P, Lin Z F and Chen S Y 2003 *Phys. Rev.* E **68** 011401
[20] Zhang C Y, Shi J, Tan H L, Liu M R and Kong L J 2004 *Chin. Phys. Lett.* **21** 1108
[21] Zhang C Y, Li H B, Tan H L, Liu M R and Kong L J 2004 *Acta Phys. Sin.* **54** 1982 (in Chinese)
[22] Zhang C Y, Tan H L, Liu M R, Kong L J and Shi J 2005 *Chin. Phys. Lett.* **22** 896
[23] Li H B, Lu X Y, Fang H P and Qian Y H 2004 *Phys. Rev.* E **70** 026701
[24] Fang H P and Chen S Y 2004 *Chin. Phys.* **13** 47
[25] Shan X and Chen H D 1993 *Phys. Rev.* E **47** 1815
[26] Guo Z L and Zhao T S 2003 *Phys. Rev.* E **68** 035302
[27] Guo Z L and Zhao T S 2005 *Phys. Rev.* E **71** 026701
[28] Swift M R, Orlandini S E, Osborn W R and Yeomans J M 1995 *Phys. Rev. Lett.* **75** 830
[29] Xu A G, Gonnella G and Lamura A 2004 *Physica* A **331** 10
[30] Xu Y S, Wu F M, Chen Y Y and Xu X Z 2003 *Chin. Phys.* **12** 621
[31] Xu Y S, Wu F M, Chen Y Y and Xu X Z 2003 *Mod. Phys. Lett.* B **19** 1351
[32] Xu Y S 2003 *Acta Phys. Sin.* **52** 626 (in Chinese)
[33] Xu Y S, Li H B, Fang H P and Huang G X 2004 *Acta Phys. Sin.* **53** 773 (in Chinese)
[34] Wu B Z, Xu Y S, Liu Y and Huang G X 2005 *Chin. Phys.* **14** 2046
[35] Fang H P, Lin Z F and Wang Z W 1998 *Phys. Rev.* E **57** **R**25
[36] Fang H P, Wang Z W, Lin Z F and Liu M R 2002 *Phys. Rev.* E **65** 051905
[37] Li H B, Fang H P, Lin Z F, Xu S X and Chen S Y 2004 *Phys. Rev.* E **69** 031919
[38] Yi H H, Xu S X, Qian Y H, Fang H P 2005 *Chin. Phys. Lett.* **22** 3210
[39] Kang X Y, Liu D H, Zhou J and Jin Y J 2005 *Chin. Phys. Lett.* **22** 2873
[40] Lu X Y, Yi H H, Chen J Y, Fang H P 2006 *Chin. Phys. Lett.* **23** 738
[41] Inamuro T, Maeba K and Ogino F 2000 *Int. J. Multiphase Flow* **26** 1981
[42] Allen M P and Tildesley D J 1987 Computer Simulation of Liquid (Oxford: Clarendon)
[43] Segré G and Silberberg A 1961 *Nature* **189** 209
[44] Segré G and Silberberg A 1962 *J. Fluid Mech.* **14** 115